



# A novel correction for biases in forest eddy covariance carbon balance

Matthew N. Hayek<sup>a,\*</sup>, Richard Wehr<sup>b</sup>, Marcos Longo<sup>c</sup>, Lucy R. Hutyrá<sup>d</sup>, Kenia Wiedemann<sup>a</sup>, J. William Munger<sup>a</sup>, Damien Bonal<sup>e</sup>, Scott R. Saleska<sup>b</sup>, David R. Fitzjarrald<sup>f</sup>, Steven C. Wofsy<sup>a</sup>

<sup>a</sup> Faculty of Arts and Sciences, Harvard University, Cambridge, MA, 02138, USA

<sup>b</sup> Department of Ecology and Evolutionary Biology, University of Arizona, Tucson, AZ, 85721, USA

<sup>c</sup> Embrapa Agricultural Informatics, Campinas, SP, Brazil

<sup>d</sup> Department of Earth and Environment, Boston University, Boston, MA, 02215, USA

<sup>e</sup> INRA, UMR EEF Université de Lorraine, INRA, 54280 Champenoux, France

<sup>f</sup> Atmospheric Sciences Research Center, SUNY Albany, Albany, NY, USA

## ARTICLE INFO

### Keywords:

Carbon dioxide  
Amazon  
Eddy covariance  
Forest carbon flux  
Respiration  
Friction velocity

## ABSTRACT

Systematic biases in eddy covariance measurements of net ecosystem-atmosphere carbon dioxide exchange (NEE) are ubiquitous in forests when turbulence is low at night. We propose an alternative to the conventional bias correction, the friction velocity ( $u_*$ ) filter, by hypothesizing that these biases have two separate, concurrent causes: (1) a subcanopy CO<sub>2</sub> storage pool that eludes typical storage measurements, creating a turbulence-dependent bias, and (2) advective divergence loss of CO<sub>2</sub>, creating a turbulence-independent bias. We correct for (1) using a simple parametric model of missing storage (MS). Prior experiments have inferred (2) directly from atmospheric measurements (DRAIN0). For sites at which DRAIN0 experiments have not been performed or are infeasible, we estimate (2) empirically using a PAR-extrapolated advective respiration loss (PEARL) approach. We compare  $u_*$  filter estimates of advection and NEE to MS-PEARL estimates at one temperate forest and two tropical forest sites.

We find that for tropical forests,  $u_*$  filters can produce a range of extreme NEE estimates, from long-term forest carbon emission to sequestration, that diverge from independent assessments and are not physically sustainable. Our MS model eliminates the dependence of nighttime NEE on  $u_*$ , consistent with findings from DRAIN0 studies that nighttime advective losses of CO<sub>2</sub> are often not dependent on the strength of turbulence. Our PEARL estimates of mean advective loss agree with available DRAIN0 measurements. The MS-PEARL correction to long-term NEE produces better agreement with forest inventories at all three sites. Moreover, the correction retains all nighttime eddy covariance data and is therefore more widely applicable than the  $u_*$  filter approach, which rejects substantial nighttime data—up to 93% at one of the tropical sites. The full MS-PEARL NEE correction is therefore an equally defensible and more practical alternative to the  $u_*$  filter, but leads to different conclusions about the resulting carbon balance. Our results therefore highlight the need to investigate which approach's underlying hypotheses are more physically realistic.

## 1. Introduction

The terrestrial CO<sub>2</sub> sink, which mitigates approximately one quarter of anthropogenic emissions, is due to an imbalance between photosynthesis, termed gross ecosystem productivity (GEP), and ecosystem respiration (R). Globally, the net ecosystem-atmosphere exchange of CO<sub>2</sub> (NEE) is less than 1% of the two gross fluxes (IPCC, 2013), with global forests representing the majority of this quantity. Much of our process-based knowledge of forest NEE is derived from eddy covariance carbon dioxide flux measurements. However, eddy covariance estimates of NEE during the nighttime (nocturnal carbon efflux or

NCE)—which represent R because photosynthesis is inactive at night—are prone to underestimation in the form of a selective systematic error (Moncrieff et al., 1996), causing an erroneous shift in the net balance towards uptake (Miller et al., 2004). Such biases in forest eddy covariance NCE therefore accumulate in the long-term ecosystem carbon balance.

The predominant explanation for the systematic low bias in NCE is that mean advective flows remove some CO<sub>2</sub> from the subcanopy air-space (Lee, 1998; Sun et al., 1998; Aubinet et al., 2003). This advective divergence loss can be caused by radiative cooling resulting in negative buoyancy, which can move cool CO<sub>2</sub>-rich air down slight slopes and

\* Corresponding author at: 24 Oxford St, Cambridge, MA 02143, USA.

E-mail addresses: [mhayek@fas.harvard.edu](mailto:mhayek@fas.harvard.edu), [nassif.hayek@gmail.com](mailto:nassif.hayek@gmail.com) (M.N. Hayek).

into the valleys (Grace et al., 1996) below eddy covariance measurement towers, which are typically placed on plateaus. These mean divergent flows violate the assumption of horizontal heterogeneity upon which the measurements rely.

Based on the assumption that calm, low-turbulence conditions facilitate the advective loss, the now ubiquitous approach to correcting NCE has been to discard nighttime eddy flux measurements when turbulence is low (Wofsy et al., 1993; Goulden et al., 1996; Gu et al., 2005; Reichstein et al., 2005; Papale et al., 2006; Barr et al., 2013). Typically, turbulence is quantified by the friction velocity ( $u_*$ ) and measurements are discarded when  $u_*$  falls below a threshold ( $u_*^{Th}$ ) below which NCE is observed to decline with  $u_*$  and above which NCE is independent of  $u_*$ . This method is referred to as the  $u_*$  filter approach.

A number of findings, however, cast doubt on the assumption that only calm, low-turbulence conditions facilitate advective divergence loss. Advective losses have been associated with negative buoyancy from thermal gradients, present even when the canopy air is turbulently mixed (Staebler and Fitzjarrald, 2005). Explicit measurements of subcanopy airflow indicate that horizontal advective divergence still occurs when  $u_*$  is much higher than the typically applied thresholds (Staebler and Fitzjarrald, 2004; Tóta et al., 2008). Furthermore, such subcanopy measurements also demonstrate that these horizontal advective fluxes do not account for the NEE correlations with  $u_*$ , and sometimes even exacerbate them (Aubinet et al., 2010). An alternative explanation for  $u_*$ -dependent biases in NCE is needed.

We propose an alternative set of hypotheses to explain the concurrent phenomena of the apparent  $u_*$ -dependence of NCE and the selective systematic error in NEE that leads to underestimation of the long-term carbon budget. The hypotheses are as follows. (1) Hidden CO<sub>2</sub> storage pools below the canopy are underestimated or unobserved by classical concentration profile measurements. The flux from the filling and emptying of these pools is dependent on  $u_*$ , and therefore accounts for turbulent-dependent biases, but cannot account for the long-term selective systematic NEE bias towards uptake. (2) Advective loss is independent of  $u_*$  but persistently occurs at night and is near zero during the day, and therefore accounts for the long-term selective systematic NEE bias towards uptake. (3) In order to estimate advective loss without explicit measurements of the phenomenon, we further hypothesize that at sunset, both nocturnal advection and photosynthesis are near zero, so eddy flux observations at this time, corrected for storage in both measured and unmeasured pools, are representative of the true  $R$ . The difference between  $R$  at sunset and  $R$  during the rest of the night therefore provides an estimate of advective loss.

Because both our hypotheses and those of the traditional  $u_*$  filter are speculative, we intend to highlight that our novel approach results in eddy flux-derived carbon fluxes that are closer to independent assessments of both advective loss and aboveground biomass changes. First, we highlight the problem by demonstrating the traditional technique of correcting NCE biases using a consistent  $u_*$  filter method across three sites (two tropical and one temperate forest). Next, we correct for a turbulence-dependent bias in NCE by modeling hypothesis (1) using a simple linear box model to compensate for effects of unmeasured CO<sub>2</sub> storage pools, which are filled or flushed depending on turbulence, but do not add or remove CO<sub>2</sub> from the system on daily or longer time-scales. We then add the mean advective loss of hypothesis (2) using prior measurements of subcanopy advection and CO<sub>2</sub> gradients at two of our three sites (Staebler and Fitzjarrald, 2004; Tóta et al., 2008). We also model the advective loss using hypothesis (3), intended for sites lacking measurements of subcanopy flow, and validate the model against the aforementioned measurements. Our approach does not discard any data and consists only of two simple, first-order data corrections, added to observations of forest NEE in sequence, that we hope will ultimately allow for accurate estimates of whole-ecosystem net CO<sub>2</sub> fluxes.

## 2. Methods

### 2.1. Measurements of carbon dioxide and aboveground woody carbon fluxes

We compared eddy flux measurements of NEE to censuses of aboveground woody increment (AGWI) at three sites: (1) the Tapajós National Forest (TNF) km67 in Pará, Brazil (Rice et al., 2004; Hutrya et al., 2007; Pyle et al., 2009), (2) Guyaflux in Paracou, French Guiana (Bonal et al., 2008; Rowland et al., 2014), and (3) the Harvard Forest in Petersham, Massachusetts, USA (Wofsy et al., 1993; Urbanski et al., 2007). Eddy flux records covered: (1) January 2002–January 2006 and August 2008–December 2011 at TNF km67, (2) 2005–2014 at Guyaflux, and (3) 1992–2013 at the Harvard Forest.

The NEE data were quality-controlled half-hourly or hourly values, calculated as the sum of the eddy flux and the measured storage flux (i.e. the rate of storage of CO<sub>2</sub> in air spaces in the subcanopy and canopy, below the eddy flux sensor height). Half-hourly values were averaged to an hourly timestep in order to have uniform minimum time steps across all three sites. The hourly NEE observations are herein referred to as NEE<sub>obs</sub>, to distinguish them from subsequent bias-corrected values. The nighttime subset of hourly NEE<sub>obs</sub> is referred to as NCE<sub>obs</sub>.

To calculate yearly and longer-timescale sums of both NEE<sub>obs</sub> and bias-corrected NEE, hourly data were gap-filled using parametric relationships of daytime NEE with photosynthetically active radiation (PAR) and air temperature (Falge et al., 2001; Dunn et al., 2007; Urbanski et al., 2007). Gap-filling was performed with independent parameters for the following seasons: wet and dry seasons at TNF km67 and Guyaflux, with each year treated independently, and 8 seasons at the Harvard Forest, with each decade treated independently. Gap-filled data were only used to produce long-term total and annual mean NEE; non-gap-filled NEE<sub>obs</sub> were used for the rest of the analysis. We estimated 95% confidence intervals due to random measurement errors for annual and total mean NEE by bootstrapping, i.e. randomly resampling (with replacement) hourly NEE<sub>obs</sub> from similar seasons, years, and PAR and temperature conditions.

Biometry censuses covered (1) 1999, 2001, 2005, and 2008–2011 for TNF km67, once per year in the early dry season, (2) 2004, 2006, 2008, and 2013 for Guyaflux, once per year in March, and (3) 1993 and 1998–2013 for the Harvard Forest, once in July 1993 and four times per year in 1998–2013. At all sites, AGWI was calculated as the annual increase in aboveground woody biomass (AGWB) in trees with diameter at breast height (DBH)  $\geq 10$  cm, plus additions from recruitment minus losses from mortality. AGWI 95% confidence intervals were produced by bootstrapping, i.e. randomly resampling yearly subplot-based sub-total AGWB with replacement in the case of TNF km67 and Guyaflux, and randomly resampling yearly total AGWI with replacement in the case of the Harvard Forest.

### 2.2. Change-point detection for a conventional $u_*$ filter approach

We applied a conventional  $u_*$  filter to NCE<sub>obs</sub> (nighttime-only NEE<sub>obs</sub>) and quantified the resulting net carbon balance in annual and long-term sums of  $u_*$  filtered NEE<sub>obs</sub>. We used the change-point detection method (CPD) for selecting  $u_*^{Th}$  due to its insensitivity to noise in the NCE vs.  $u_*$  relationship and its prior validation at a suite of 38 North American forest eddy covariance sites (Barr et al., 2013). The CPD method consists of two steps: (1) binning the NCE<sub>obs</sub> and  $u_*$  data into  $n_B$  equally sized  $u_*$  classes and (2) modeling the response of binned NCE<sub>obs</sub> vs.  $u_*$  as two intersecting linear regressions, with their intersection representing the threshold,  $u_*^{Th}$ , below which data are discarded.

For each site, we modified step (1) from the original CPD method by binning NCE<sub>obs</sub> and  $u_*$  for all years, instead of each individual year. Results were robust to a large range of values for  $n_B$ , but we selected a value of  $n_B = 500$  for every site to allow our binning to include

substantial information in the long tail of the  $u_*$  distribution. For step (2), Barr et al. (2013) included two versions of the change-point regression approach in their analysis: one for which the second regression has a fitted slope (increasing or decreasing high- $u_*$  response), and another for which the slope is simply zero (no high  $u_*$  response). For parsimony, we used the second approach for all sites. Their CPD model is:

$$NEE_{obs, i} = \begin{cases} a_0 + a_1 u_{*i} + \varepsilon, & 1 \leq i \leq c \\ a_0 + a_1 u_{*c} + \varepsilon, & c \leq i \leq n \end{cases} \quad (1)$$

where  $i$  is a discrete index of the independent variable  $u_*$  to ensure that the intersection between the two linear regressions lies within the interval between  $i = 1$  and  $i = n$ . The fitted linear regression parameters  $a_1$  and  $a_0$  are calculated for each value of  $u_*$  change points  $u_{*c}$  from  $c = 2$  to  $c = n - 1$ . The most probable value of  $u_{*c}$  is the one that minimizes the sum of squared errors for its respective double regression. We set this value of  $u_{*c}$  to be our final  $u_*^{Th}$ . Errors in  $u_*^{Th}$  are reported as 95% confidence intervals, generated by bootstrapping: we randomly sampled pairwise  $NCE_{obs} - u_*$  observations with replacement and regenerated regressions for 501 simulations, recalculating  $u_*^{Th}$  for each simulation. Using the CPD technique for  $u_*^{Th}$  detection allowed us to apply a consistent, conventional  $u_*$  filter approach to  $NCE_{obs}$  from disparate forest sites.

The CPD is not the only  $u_*$  filter selection algorithm; the debate between which algorithm is most prudent is still active (Barr et al., 2013; Galvagno et al., 2017). To present the full ranges long-term carbon balance with respect to various  $u_*$  filters, we used a spectrum of  $u_*$  thresholds at each site to recalculate annual and long-term total  $NEE_{obs}$ :  $u_*^{Th} = 0, 0.1, 0.2, 0.3, 0.4$ , the commonly used literature  $u_*^{Th}$  value, and our CPD  $u_*^{Th}$  calculation from Eq. (1). In the case that our CPD  $u_*^{Th}$  result agreed with the literature  $u_*^{Th}$  value within 95% confidence intervals, we used the literature  $u_*^{Th}$  value to produce results consistent with previous studies. Using a wide range of  $u_*^{Th}$  values allowed us to demonstrate how using any type of  $u_*$  filter, not merely the CPD, compares with our alternative correction, which is described in the following sections.

### 2.3. An alternative correction: MS-PEARL

Our full correction takes the form of two addends to standard measurements of forest  $NEE_{obs}$ :

$$NEE = NEE_{obs} + \frac{dC_2(u_*, t)}{dt} + A(t); \quad NEE_{obs} = fCO_2 + \frac{dC_1}{dt} \quad (2)$$

where  $fCO_2$  is the measured eddy covariance turbulent flux and  $dC_1/dt$  is the measured canopy storage flux, i.e. the time derivative of column weighted average of  $CO_2$  concentration measurements, denoted here as  $C_1$ . We add two corrective modeled terms to address biases in  $NEE_{obs}$ :  $dC_2/dt$  is the unmeasured “missing storage” (MS) flux not captured by measurements of  $dC_1/dt$ , and  $A(t)$  is the mean advective divergence loss.

Our MS flux model is described in Section 2.3.1. The MS term is intended to correct for the turbulent-dependent biases in  $NEE_{obs}$ , which includes the classical storage column measurement. Our MS flux model is agnostic to where the missing storage pool is located. We offer three hypotheses for the location of this pool, which are not mutually exclusive: (1) a horizontally disparate location, outside of the  $CO_2$  storage column measurement footprint, but within the relatively large footprint of the above-canopy eddy flux sensor, (2) the airspace above the leaf litter layer but below the lowest  $CO_2$  profile measurement inlet (typically  $> 0.5$ – $1.0$  m above the ground), or (3) the soil pore and leaf litter airspace. Regarding the first hypothesis, we note that flux towers are necessarily located in canopy gaps, and so  $CO_2$  storage in dense canopies may be greater than estimated from measurements on a tower. Identifying the location(s) of the MS pool, however, is outside of the

scope of this study; we intend for our hypotheses to serve as an outline for future investigations.

Our modeled advective loss estimate  $A$  is described in Section 2.3.2. We modeled advective loss as turbulence-independent, intending to correct the selective systematic bias that affects long-term NEE (Moncrieff et al., 1996), which likely results from nighttime drainage flows. We also present a summary of prior measurements of advective loss at two of our study sites in Section 2.3.2. Studies suggest that advective loss is primarily related to atmospheric buoyancy (Staeble and Fitzjarrald 2004; van Gorsel et al., 2007; Tóta et al., 2008), not boundary layer turbulence. However instead of modeling the quantitative relationship between potential temperature and advection, we simply utilize the ensemble mean  $A$  across multiple years for nighttime hours, and assume it is absent at daytime.

#### 2.3.1. Correcting for missing storage (MS)

We developed a simple parametric box model of the unobserved MS flux,  $dC_2/dt$ . The flux is positive, negative, or zero depending on the turbulent conditions in that hour and on the accumulated concentration in the previous hour:

$$\frac{dC_2(t_i)}{dt} = \begin{cases} R_2 - \alpha u_*(t_i) & \text{if } \frac{C_2(t_{i-1})}{t_i - t_{i-1}} + R_2 > \alpha u_*(t_i) \\ \frac{C_2(t_{i-1})}{t_i - t_{i-1}} & \text{if } \frac{C_2(t_{i-1})}{t_i - t_{i-1}} + R_2 \leq \alpha u_*(t_i) \end{cases} \quad (3)$$

$C_2$  represents the hourly  $CO_2$  concentration enhancement above  $C_1$ ; it is a height-integrated concentration quantity in units of  $\mu\text{mol m}^{-2}$ .  $C_2$  is time-integrated across one hourly timestep ( $t_i - t_{i-1}$ , expressed in seconds to keep units consistent) once the MS flux into or out of the pool is calculated. By definition,  $C_2$  cannot go below 0, a condition which represents full mixing with the  $C_1$  pool. The two free parameters,  $R_2$  and  $\alpha$ , are time-invariant.  $R_2$  is the amount of total ecosystem respiration flux that does not immediately end up in observations of  $C_1$  or  $fCO_2$  in that hour, because it accumulates in the unmeasured storage pool.  $\alpha$  is the mixing concentration in units of  $\mu\text{mol m}^{-3}$  that, when multiplied by  $u_*$ , produces the flushing rate of the unmeasured storage pool. As noted earlier, a precise physical interpretation depends on which hypothesis regarding the location of the MS pool is correct, a question that is outside the scope of this study.

Our MS model parameters,  $R_2$  and  $\alpha$ , were fit as follows: for each site, all combinations of the two parameters, rasterized over a range of values, were tested.  $R_2$  and  $\alpha$  ranged between 0 and  $6 \mu\text{mol m}^{-2} \text{s}^{-1}$  and  $0$ – $40 \mu\text{mol m}^{-3}$ , respectively, at discrete intervals of  $0.1 \mu\text{mol m}^{-2} \text{s}^{-1}$  and  $1 \mu\text{mol m}^{-3}$ , respectively. For every parameter combination in these ranges, the MS model (Eq. (3)) was run from an initial value of  $C_2(t_0) = 0$  in a time-forward manner across the entire eddy flux time series. The cost function was then calculated for the nighttime subset of values. Our cost function was based on the hypothesis that the  $u_*$  dependency in the nighttime flux ( $NCE_{obs}$ ) is solely due to MS flux, not advection or any biological process. Because MS-corrected  $NCE_{obs}$  should have minimal  $u_*$  dependence at night, our optimization takes the form of minimizing the root mean squared deviation of residual MS-corrected  $NCE_{obs}$  around the sample mean value:

$$\min(RMSD(NCE_{obs} + \frac{dC_2}{dt} - \overline{NCE_{obs} + \frac{dC_2}{dt}})) \quad (4)$$

The optimization was intended to find which parameter values resulted in the “flattest”  $NCE_{obs} + MS$  vs.  $u_*$  relationship, in hopes that the functional form of Eq. (3) could result in a substantial flattening and not a minor one. The combination of parameter values within the raster grid that minimized the cost function for each site were thus taken as the final MS model parameter values, and the MS model was applied to the full  $NEE_{obs}$  time series.

#### 2.3.2. Correcting for advective loss (DRAIN and PEARL)

We assume advection is simply constant and positive during the

night and zero during the day:

$$A(t) = \begin{cases} A_{\text{night}}, & \text{night} \\ 0, & \text{day} \end{cases} \quad (5)$$

In actuality, advection is likely dependent upon thermal buoyancy (Staebler and Fitzjarrald, 2004), but this relationship was not included due to lack of constraint.

At the Harvard Forest and TNF km67 sites, an array of subcanopy measurements of wind speed and  $\text{CO}_2$  were deployed in previous studies to estimate the horizontal and vertical advective divergence of  $\text{CO}_2$  from the subcanopy airspace (Staebler and Fitzjarrald, 2004; Tóta et al., 2008). These experiments were dubbed the DRAINO experiments. At both DRAINO sites, exploratory observation campaigns were conducted before primary measurements to determine an optimal sensor network configuration and to characterize the dominant subcanopy flow characteristics. Points of measurement in the subcanopy airspace were made on the corners and edges of a square control area surrounding the tower. Quantifying the spatial scales of advection and  $\text{CO}_2$  concentration gradients, as well as the effect size of drag from subcanopy stem density, allowed for the determination of optimal horizontal spacing and orientation of sensors as well as their height, necessary for counteracting the expected small signal-to-noise ratio. Nocturnal flows were also related to physical forcing characteristics below the subcanopy to ensure that they were systematic. The DRAINO measurement campaigns at both sites were able to quantify the transport of  $\text{CO}_2$  out of the control volume by identifying the horizontal advective divergence loss process. Both studies reported mean and standard errors for their  $A_{\text{night}}$  estimates. We used the mean nighttime advection for  $A_{\text{night}}$  from the multi-year DRAINO campaigns at both sites (growing season only for the Harvard Forest). We call the full NEE correction (Eq. (2)) using the DRAINO-derived estimate for  $A_{\text{night}}$  the MS-DRAINO correction.

Subcanopy measurements of a control volume of airspace beneath eddy covariance towers such as those in the DRAINO campaigns are labor-intensive and costly. Therefore, we devised a method for estimating the advective loss, which we call the PAR-extrapolated advective respiration loss (PEARL). This technique exploits the facts that (1) there is a time delay between nightfall and the onset of thermal gradients that stably stratify the subcanopy airspace and advect  $\text{CO}_2$  away from the flux apparatus (van Gorsel et al., 2007) and (2) after correcting for the missing storage flux,  $\text{NCE}_{\text{obs}} + \text{MS}$  in the first hour tends to be higher than the rest of the night.

Our PEARL approach for deriving  $A_{\text{night}}$  from  $\text{NEE}_{\text{obs}} + \text{MS}$  builds on that devised by van Gorsel et al. (2008), who found that the first few hours of the night had more positive  $\text{CO}_2$  fluxes. They concluded that this early night “bump” was reflective of the true respiration  $R$  because the atmosphere remained thermally buoyant and advective loss was insignificant. Our approach builds on theirs with two important

additions: (1) we first corrected  $\text{NEE}_{\text{obs}}$  by MS, and found that the bump was present or more prominent after the correction (2) we did not make any assumptions about the precise length of time between sunset and the onset of nocturnal advection (e.g. that it was exactly one hour, the time resolution of our flux measurements, or multiple hours). Instead of identifying the early night bump in time space, we opted for PAR space, taking the limit of evening  $\text{NEE}_{\text{obs}} + \text{MS}$  to zero PAR as an approximation of the true  $R$  absent any advective loss:

$$R = \lim_{\substack{\text{PAR} \rightarrow 0 \\ T \rightarrow T_{\text{night}}}} (\text{NEE}_{\text{obs}} + \frac{dC_2}{dt}) = a_1 + a_2 T + \frac{a_3 \cdot \text{PAR}}{a_4 + \text{PAR}} \quad (6)$$

where  $\text{NEE}_{\text{obs}}$  is the observed NEE,  $T$  is air temperature,  $dC_2/dt$  is the MS flux, modeled in Section 2.3.1, and  $a_2$  is the temperature sensitivity parameter separately fit to the nighttime data. We fit the curve using nonlinear least squares regression for  $\text{NEE}_{\text{obs}} + \text{MS}$  past noon and a lower PAR threshold of  $\text{PAR} > 0 \mu\text{mol m}^{-2} \text{s}^{-1}$  to utilize evening values as close as possible to sundown. We used an upper PAR threshold of  $\text{PAR} < 1000 \mu\text{mol m}^{-2} \text{s}^{-1}$  so that the regression fit was insensitive to the functional form of the high-PAR curvature—hyperbolic, logarithmic, or quadratic—all of which we tested for TNF km67 and include in the discussion of our results. At the tropical sites, we assume  $a_2 = 0$  because temperature variability is too small to allow for detection of significant hourly sensitivity (Hutyra et al., 2007).

After fitting the evening PAR curve, the nighttime  $R$  equals  $a_1 + a_2 \text{mean}(T_{\text{night}})$ , where  $T_{\text{night}}$  is the nighttime temperature. Overbars denote long-term averages. Lastly, subtracting the mean MS-corrected  $\text{NCE}_{\text{obs}}$  from the evening-extrapolated estimate for  $R$  provides the PEARL estimate for nighttime advection  $A_{\text{night}}$ :

$$a_1 + a_2 \overline{T_{\text{night}}} - (\overline{\text{NCE}_{\text{obs}}} + \frac{dC_2}{dt}) = A_{\text{night}} \quad (7)$$

We added the MS and PEARL corrections to  $\text{NEE}_{\text{obs}}$  and reapplied gap filling to the entire time series at the tropical sites, km67 and Guyaflux, and to the growing season at the temperate site, the Harvard Forest. We call the overall correction using PEARL the MS-PEARL correction.

### 3. Results and discussion

#### 3.1. Eddy flux carbon balance from $u_*$ filters

We applied CPD to the binned  $\text{NCE}_{\text{obs}}$  vs.  $u_*$  relationship of all three sites to assess the carbon balance resulting from a conventional  $u_*$  filtering approach (Fig. 1). Results for  $u_*^{\text{Th}}$  detected by CPD are in Table 1. For both the Harvard Forest (growing season only) and Guyaflux sites,  $u_*^{\text{Th}}$  from CPD agreed with the commonly used literature values within

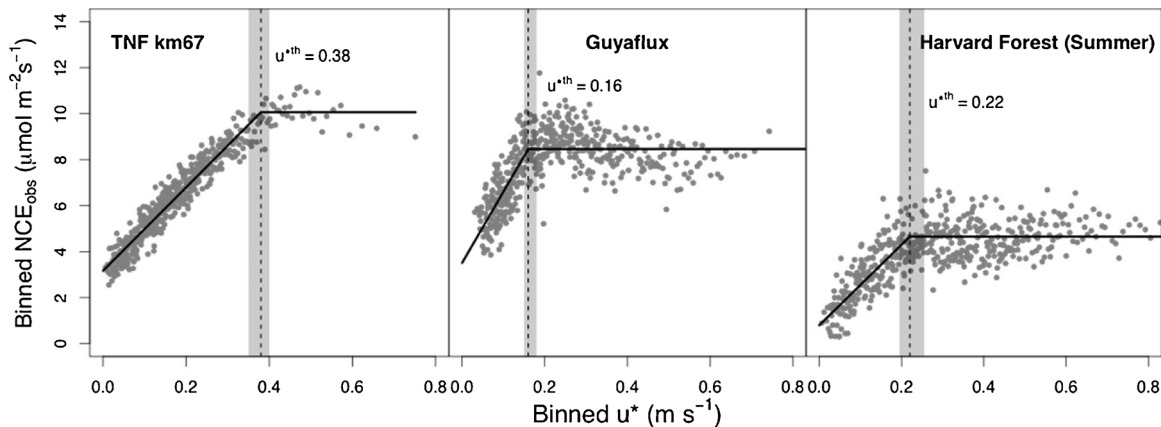


Fig. 1. Binned NCE by equally sized  $u_*$  classes ( $N_B = 500$ ). Solid black line is the best-fit change-point regression from Eq. (1). Vertical dotted line is the CPD detected  $u_*^{\text{Th}}$ . Shaded area is the 95% confidence interval of CPD  $u_*^{\text{Th}}$ .



**Table 1**

Literature and CPD  $u_*^{Th}$ , with the resulting CPD  $u_*^{Th}$  advective loss and carbon balance. NEP and AGWI have the same sign convention (NEP =  $-NEE$ ): positive corresponds to net carbon accrual and negative corresponds to carbon loss. For Harvard Forest, the summer  $u_*^{Th}$  was applied to NEP for the entire year. 95% confidence intervals are in parentheses.

Site	Lit.	CPD				Mean annual AGWI (MgC ha <sup>-1</sup> y <sup>-1</sup> )
	$u_*^{Th}$ (m s <sup>-1</sup> )	$u_*^{Th}$ (m s <sup>-1</sup> )	NCE data remaining	Advective loss ( $\mu\text{mol m}^{-2} \text{s}^{-1}$ )	Mean annual NEP (MgC ha <sup>-1</sup> y <sup>-1</sup> )	
TNF km67	0.22	0.38 (0.34, 0.40)	7%	3.95 (3.63, 4.01)	-4.42 (-5.07, -3.87)	0.39 (-1.29, 2.12)
Guyaflux	0.15	0.16 (0.15, 0.18)	60%	0.42 (0.40, 0.45)	3.49 (3.29, 3.69)	-0.46 (-2.12, 1.04)
Harvard Forest (summer)	0.20	0.22 (0.19, 0.26)	59%	0.73 (0.69, 0.75)	2.96 (2.88, 3.04)	1.60 (-1.43, 1.76)

the 95% confidence intervals (Urbanski et al., 2007; Bonal et al., 2008). At TNF km67, CPD found  $u_*^{Th} = 0.38 \text{ m s}^{-1}$ , which is significantly greater than the commonly used literature value of  $u_*^{Th} = 0.22 \text{ m s}^{-1}$  (Saleska et al., 2003; Hutrya et al., 2007; Hutrya et al., 2008). The full 7.5 year record of NCE does not demonstrate a plateau at  $u_* = 0.22$  (Fig. 1). CPD  $u_*^{Th}$  was not consistent with the literature  $u_*^{Th}$ , but was consistent with published findings that NCE still demonstrated turbulence dependence well above  $u_* = 0.22 \text{ m s}^{-1}$  (Saleska et al., 2003; Hutrya et al., 2007). The literature  $u_*^{Th}$  was determined by using a four-month to one-year long subset of the NCE and  $u_*$  data (Saleska et al., 2003; Hutrya et al., 2008). Using CPD  $u_*^{Th}$  to filter NCE left only 7% of NCE available for estimating nighttime respiration. There were no unfiltered nighttime hours remaining in some months. At the Harvard Forest, CPD could not detect a  $u_*$  threshold for wintertime data (Fig. S1); we therefore applied the summertime filter to the entire eddy flux time series at this site.

The mean  $R$  at TNF km67 resulting from the CPD  $u_*^{Th}$  filter was  $10.06 \mu\text{mol m}^{-2} \text{s}^{-1}$ , which resulted in a strong net source of  $4.42 \text{ MgC ha}^{-1} \text{y}^{-1}$ . Both Guyaflux and the Harvard Forest were significant sinks after applying the CPD  $u_*^{Th}$  filter, consistent with previously reported  $u_*$  filtered results (Table 1). Mean  $R$  at Guyaflux resulting from the CPD  $u_*^{Th}$  filter was  $8.13 \mu\text{mol m}^{-2} \text{s}^{-1}$ , which resulted in a large net sink of  $3.49 \text{ MgC ha}^{-1} \text{y}^{-1}$  (Table 1).

All three sites had a resulting carbon balance ( $NEP_{\text{obs}} = -NEE_{\text{obs}}$ ) that was significantly different from the mean AGWI (Table 1). Furthermore, the net carbon source at TNF km67 resulting from the CPD  $u_*^{Th}$  filter is unsustainably high; based on biomass carbon stocks estimates from Malhi et al. (2009), such emissions would result in no remaining forest biomass after 62 years. The forest was not anomalously stressed during the decade of measurements: the interannual variability in precipitation and temperature was well within the multi-decadal historical interannual variability (Hayek, 2017), making such a strong source of  $\text{CO}_2$  unlikely at TNF km67. Similarly, at Guyaflux, the strength of the net carbon sink was unsustainable, resulting from the CPD  $u_*^{Th}$  filter would result in a doubling of forest biomass over 81 years.

The TNF km67 site showed the greatest sensitivity amongst the three sites to the choice of  $u_*^{Th}$ : the range of gap-filled  $NEE_{\text{obs}}$  corresponding to  $0 \leq u_*^{Th} \leq 0.4 \text{ m s}^{-1}$  was  $8.1 \text{ MgC ha}^{-1} \text{y}^{-1}$  at km67 (Fig. 2),  $1.5 \text{ MgC ha}^{-1} \text{y}^{-1}$  at Guyaflux, and  $1.3 \text{ MgC ha}^{-1} \text{y}^{-1}$  at the Harvard Forest (Fig. S2). The km67 carbon balance ranged from a significant sink to a source, while the carbon balance at Guyaflux was a significant sink regardless of the  $u_*$  filter.

Filtering data by using a different proxy for nighttime turbulence did not improve the carbon balance estimate. The recommendation by Acevedo et al. (2009) to use the standard deviation of vertical velocity fluctuations ( $\sigma_w$ ) instead of  $u_*$  resulted in an even higher plateau of NCE at TNF km67 ( $10.63 \mu\text{mol m}^{-2} \text{s}^{-1}$ ), hence a stronger net  $\text{CO}_2$  source. The  $u_*$  filtered Guyaflux NEE was a strong sink of carbon, despite the AGWI over a similar time period being insignificantly different from zero (Table 1) and additional carbon reservoirs in this forest also

showing little to no net accumulation of carbon (Rowland et al., 2014). We conclude that  $u_*$  filters potentially bias NEE, and may lead to unreasonable hourly and seasonal nighttime  $R$  rates and unsustainable long term net carbon budgets at the tropical forest sites.

### 3.2. Missing storage model

We optimized the parameters of the MS model according to Eqs. (3) and (4). Results for the optimized MS parameters are in Table 2. The behavior of the MS pool,  $C_2$ , over time is demonstrated for 5 days in the 2005 wet season at TNF km67 as an example case in Fig. 3. The resulting modeled storage pool  $C_2$  tends to accumulate  $\text{CO}_2$  at night when  $u_*$  is low, and flushes in the morning as  $u_*$  increases, until reaching the zero constraint. The time series demonstrates variability in the accumulation and flushing of the  $C_2$  pool across different nights as  $u_*$  varies.

At each site, a single MS parameter optimization solution was found for the minimum deviation in hourly  $NCE_{\text{obs}} + MS$  from its mean value (Fig. 4; Table 2). The modeled MS flux has two regimes: accumulation ( $au_* < R_2$ ) and flushing ( $au_* > R_2$ ). In the accumulation regime, the MS flux is positive and decreases linearly with increasing  $u_*$ . This always corresponds to the first condition in Eq. (3). In the flushing regime, the opposite is true: the output exceeds the input. One of two extreme scenarios typically occurs during flushing regime hours. (1) If  $C_2$  was large enough in the previous hour to support flushing, the MS flux is negative and lands on the same MS vs.  $u_*$  line as the accumulation regime. This also corresponds to the first condition of Eq. (3). (2) If  $C_2$  in the previous hour was zero or lower than the net flushing, then  $C_2$  hits the boundary condition of complete mixing, because any input is immediately flushed out within that hour. This scenario corresponds to the second condition in Eq. (3), leading to weakly negative or zero net MS flux.

The resulting binned MS-corrected NCE at all three sites is presented in Fig. 5. The MS model offers an alternative explanation of the  $u_*$  change point tendency in  $NCE_{\text{obs}}$  (Fig. 1). Guyaflux and Harvard Forest have higher flushing rates  $\alpha$  and higher mean  $u_*$  than TNF km67, and therefore attain the zero-boundary flushing scenario more frequently (Table 2), resulting in lower- $NCE_{\text{obs}}$  plateaus and fewer pronounced negative flushing rates (Fig. 4, light grey triangles). The MS model can therefore account for changes in the shape of the  $NCE_{\text{obs}}$  vs.  $u_*$  relationship between sites.

The MS flux diel pattern is synchronous and correlated with that of the measured storage flux (Fig. 6). Like the measured storage, MS is a zero-mean process over an average diurnal cycle.  $NEE_{\text{obs}} + MS$  shows both higher nighttime emission and higher daytime uptake than the original NEE. Thus, the gap-filled  $NEE_{\text{obs}} + MS$  has the same mean annual total as gap-filled  $NEE_{\text{obs}}$  without any  $u_*$  filter.

At all three sites, the first hour of nighttime  $NEE_{\text{obs}} + MS$  exhibits the highest positive flux (Fig. 6). This early nighttime “bump” was also detected in  $NEE_{\text{obs}}$  by van Gorsel et al. (2008) at a eucalyptus forest site and was used to infer the nighttime advective loss.

To elucidate the physical location of the MS pool, for which we

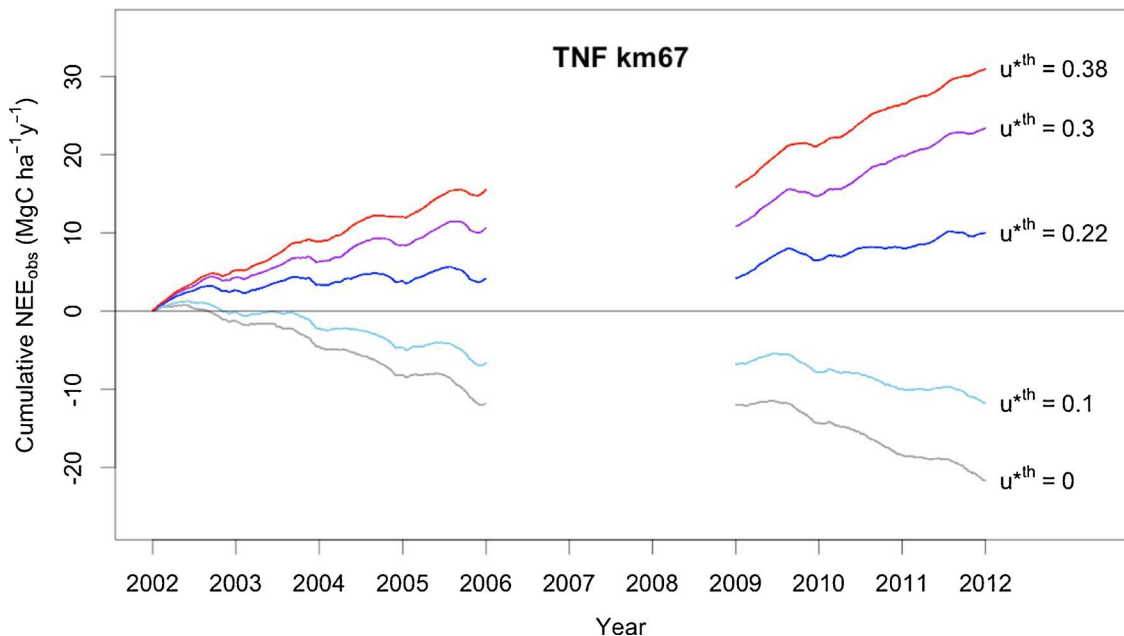


Fig. 2. TNF km67 net cumulative carbon balance from January 1, filtered by various  $u_*^{th}$ . The cumulative sum was not reset during the 2006–2008 gap.

presented some hypotheses in Section 2.3, additional analyses of pre-existing measurements and novel measurement campaigns in the sub-canopy airspace are needed. As an example, novel profile column measurements, located in the eddy flux footprint but without the gap associated with an eddy covariance tower, could be used to test hypothesis 1. Additionally, to test hypothesis 2, data from short sub-canopy profile towers near the forest floor collected at TNF km67 and Harvard Forest as part of the respective DRAINCO campaigns (Staebler and Fitzjarrald, 2004; Tóta et al., 2008), may be used to test whether near-ground accumulation is greater than that in lowest standard profile measurement ( $< 0.5\text{--}1.0\text{ m}$ ). Lastly, if the MS pool is instead located within the leaf litter and soil pore space (hypotheses 3), then the MS parameter  $R_2$ , our box model input rate, may be approximately equivalent to  $R_{soil}$ . Indeed,  $R_{soil}$  is approximately  $4\text{ }\mu\text{mol m}^{-2}\text{s}^{-1}$ , similar to  $R_2$ , at TNF km67 and at Harvard Forest during the summer (Hutyra et al., 2008; Giasson et al., 2013). However, estimates of  $R_{soil}$  may also be affected by turbulence and wind biases due to pressure differentials at chamber vents (Gu et al., 2002; Bain et al., 2005), imparting  $R_{soil}$  with the similar biases to those of  $NCE_{obs}$ . Additional modeling of this process may therefore be needed. Testing the various physical hypotheses is further complicated by the fact that the MS pool may have more than one physical location.

A foundational assumption of our MS model is that all unmeasured storage can be treated as a single pool on average, with one accumulation and one flushing rate. This assumption is likely violated at tropical sites with far more heterogeneous and complex terrain directly adjacent to the tower (Tóta et al., 2012) and at the Harvard Forest in the dormant season, providing qualitatively different correlations between  $NCE_{obs}$  and  $u_*$  (Fig. S1). Harvard Forest winter  $NCE_{obs}$  did not exhibit a high- $u_*$  plateau. In contrast to winter  $NCE_{obs}$ , winter daytime  $NEE_{obs}$  increased more rapidly with  $u_*$  as  $u_*$  increased. Differences between the summer and winter  $NCE_{obs}$  vs.  $u_*$  curves are likely related to

the winter absence of a forest canopy, which has a peak summer leaf area index of 5 (Urbanski et al., 2007). We excluded Harvard Forest dormant season from our analysis because three factors would require a more sophisticated MS model: (1) during the dormant season, leaf loss causes profile measurement-sensed airspace to ventilate easily; (2) leaf shedding adds a thick leaf litter layer seal to the forest floor, beneath which storage measurements are not present; (3) snowfall adds an additional barrier in the winter. Nonetheless, our MS model accounted for and corrected the slope-plateau behavior of  $NCE_{obs}$  at times of the year when the forest canopy was foliated at all sites.

### 3.3. The PEARL advection correction

#### 3.3.1. PEARL estimates of advective loss

We estimated  $A_{night}$  (Eq. (5)) using the PEARL approach (Eqs. (6)–(7)), illustrated for TNF km67 in Fig. 7. We compared PEARL  $A_{night}$  with that from DRAINCO experiments under the assumption that these advection measurements are a reliable indication of the mean  $A_{night}$  for the entire time series. We found that PEARL agreed with measurements from both DRAINCO sites within literature-reported DRAINCO mean standard errors and PEARL 95% mean confidence intervals (Table 3).

We note that advective losses in physical systems may not correspond precisely to the assumption of zero  $u_*$  dependency in  $A_{night}$ . For example, Tóta et al. (2008; Fig. 13 therein) still demonstrate a negative dependency of advective loss upon  $u_*$ . The effect size of this dependency is weaker than that in  $NEE_{obs}$  (Fig. 1). Through a portion of the  $u_*$  range,  $u_* = 0.15$  to  $u_* = 0.35\text{ m s}^{-1}$ , there was no association or even a slight positive association with  $u_*$  instead of the presupposed negative association. We inspected the TNF km67 data and found that this  $u_*$  range actually represents a majority of nighttime hours, about 55%, because turbulence infrequently reaches values of  $0.4\text{ m s}^{-1}$  or greater at this site (Fig. 1). An association between  $A_{night}$  and  $u_*$  is

Table 2  
Parameters for MS model.

Site	$R_2$ ( $\mu\text{mol m}^{-2}\text{s}^{-1}$ )	$\alpha$ ( $\mu\text{mol m}^{-3}$ )	Mean nighttime $u_*$ ( $\text{m s}^{-1}$ ) ( $\pm$ SD)	Proportion of nighttime flushing hours when $dC_2/dt = 0$
TNF km67	4.7	18	0.19 ( $\pm$ 0.11)	20.8%
Guyaflux	4.2	26	0.21 ( $\pm$ 0.14)	80.7%
Harvard Forest (summer)	4.5	22	0.31 ( $\pm$ 0.19)	86.6%

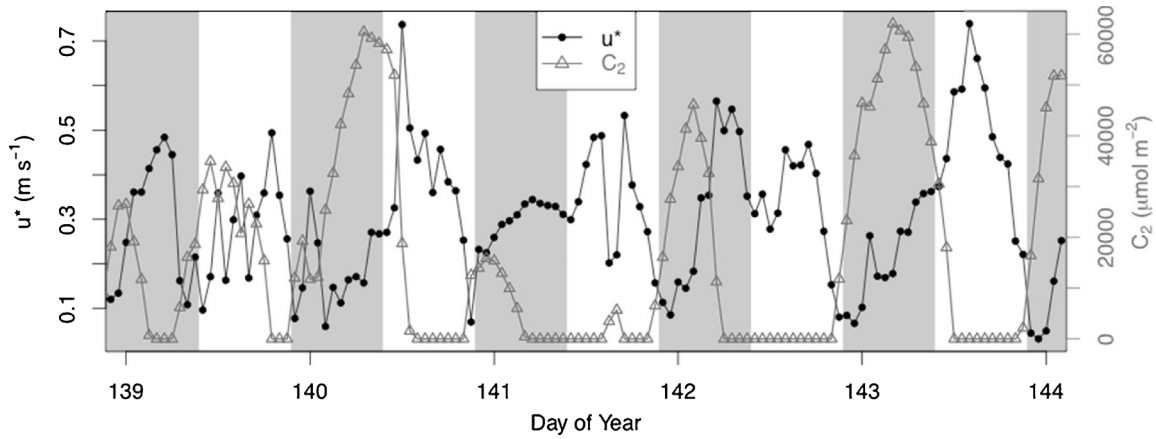


Fig. 3. Example of the hourly time series of missing storage pool concentration enhancement  $C_2$  (grey triangles) plotted with  $u^*$  time series (black dots) for TNF km67 from May 18–24, 2005. Light grey shaded areas are nighttime hours.

therefore not mutually exclusive with MS accounting for the majority of the variation in  $NEE_{obs}$  with respect to  $u^*$  (Fig. 5).

More challenging, however, is that Aubinet et al. (2010) show a number of biases associated with DRAIN-like measurements of horizontal and vertical advection, including varying directions of  $u^*$  dependency, over- or under-compensation of a realistic nighttime flux magnitude, and varying correction magnitudes from different wind sectors. We note, however, that these campaigns lacked the exploratory observations that were performed in DRAIO campaigns to determine optimal site-specific physical network configuration. Additionally, the DRAIN campaigns sought to link the subcanopy flow processes to physical forcing, ensuring that transport processes were systematic. The lack of site-specific exploratory observations, performing measurement network design testing, and linking advective flows to physical conditions may have played a role in not allowing Aubinet et al. (2010) to determine consistent advective losses across forest sites with vastly different physical structure and terrain. The DRAIN advective loss estimates were persistent across multiple years of measurement and of significant importance. We therefore believe the DRAIN results represent robust estimates of advective loss with which to compare our empirical PEARL estimates.

Uncertainties in PEARL  $A_{night}$  arise from the choice of the nonlinear functional form and of the upper PAR bound for the regression. At TNF km67, various choices of upper PAR threshold (from 300 to 2000  $\mu\text{mol m}^{-2}\text{s}^{-1}$ ), and various functional forms for  $NEE_{obs} + MS$  vs. PAR (logarithmic, hyperbolic, and quadratic), resulted in a range of approximately  $\pm 0.15 \mu\text{mol m}^{-2}\text{s}^{-1}$  in  $A_{night}$ , which is similar to our estimated random error. We opted for a less extreme upper threshold of  $PAR = 1000 \mu\text{mol m}^{-2}\text{s}^{-1}$  because the resulting PEARL  $A_{night}$  estimate

was less sensitive to the choice of regression function when very high-PAR curvature was excluded. Because our lower PAR threshold of zero allowed us to evaluate the PAR-curve intercept with plenty of data near the nighttime limit, our PEARL estimates of  $A_{night}$  were robust.

A potential systematic bias in PEARL  $A_{night}$  might arise from diurnal hysteresis in  $R_{soil}$ , which is greater earlier in the night than later, even after accounting for temperature variation. However, the diurnal hysteresis in  $R_{soil}$  could be due to physical time delays, associated with molecular and thermal diffusion, and not biological ones (Phillips et al., 2011). If this hypothesis is correct, then the hysteresis in  $R_{soil}$  is likely already subsumed by MS, which accounts for diurnal hysteresis in efflux of total  $R$  (Fig. 6) via minimizing the nighttime variance  $NCE_{obs} + MS$  (Eq. (4)). Alternatively, supposing that the hysteresis in  $R_{soil}$  is biological, Phillips et al. (2010) quantified the magnitude of this hysteresis for Harvard Forest. They found that, while the diel hysteresis in  $R_{soil}$  can be large (up to multiple  $\mu\text{mol m}^{-2}\text{s}^{-1}$ ), the magnitude of the difference over the course of the night is on the order of  $0.3 \mu\text{mol m}^{-2}\text{s}^{-1}$ , well below our Harvard Forest PEARL estimate of  $1.69 \mu\text{mol m}^{-2}\text{s}^{-1}$  (Fig. S3). We also ruled out additional biases in PEARL  $A_{night}$  such as the Kok effect of diminishing daytime plant respiration because these effects vanish at our minimum PAR threshold of zero (Bruhn et al., 2011; Heskel et al., 2013). Consistent with the findings of van Gorsel et al. (2008), we conclude that nighttime changes in  $R_{soil}$  are likely small relative to our estimates of  $A_{night}$ .

### 3.3.2. Total MS-PEARL eddy flux carbon balance correction

We inserted our PEARL  $A_{night}$  into our total correction for  $NEE$  (Eq. (2)). The mean annual  $NEE_{obs} + MS$ -PEARL for all three sites are presented in Fig. 8, integrated annually and averaged for all years in the

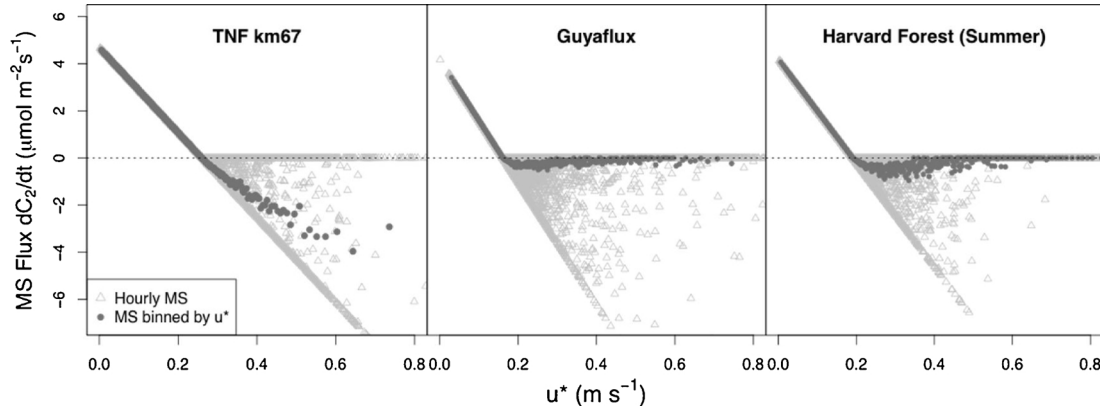
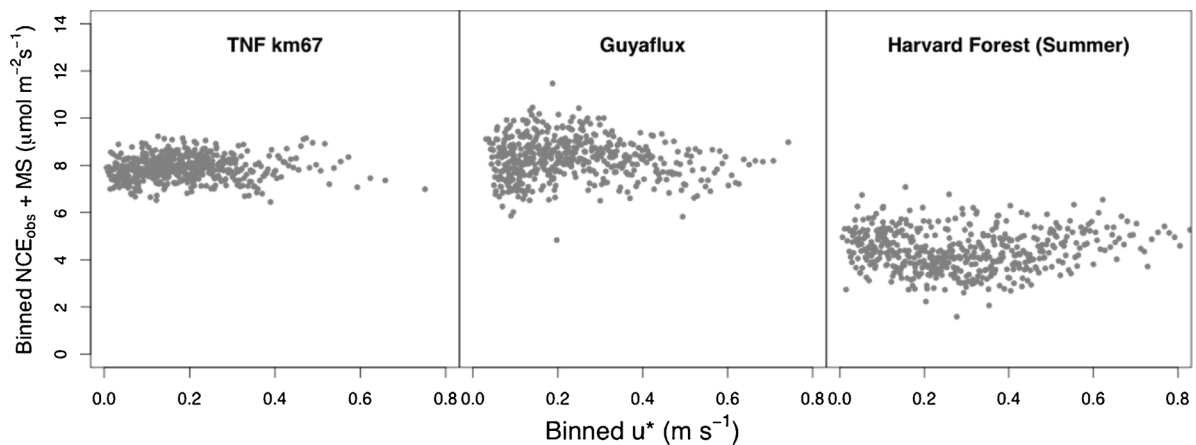


Fig. 4. Modeled MS vs.  $u^*$ , hourly (light grey triangles) and binned by equally sized  $u^*$  classes, as in Fig. 1 (dark grey circles). Positive values are accumulation and negative are flushing.

Fig. 5. Binned MS-corrected NCE vs.  $u_*$ .

time series, presented in units of  $\text{MgC ha}^{-1} \text{yr}^{-1}$ . At both tropical sites,  $\text{NEE}_{\text{obs}} + \text{MS}$ -PEARL was within the 95% confidence intervals of the mean annual AGWI from forest biometry. The uncorrected  $\text{NEE}_{\text{obs}}$  and CPD  $u_*$ -filtered  $\text{NEE}_{\text{obs}}$  were significantly different from AGWI (Fig. 8; Table 3). At Harvard Forest, the MS-PEARL correction moved NEE only partially closer to AGWI, but the correction was only applied to the growing season.

The sign of the Guyaflux AGWI and  $\text{NEE}_{\text{obs}} + \text{MS}$ -PEARL are opposite, although most of the net AGWI loss stemmed from a single large mortality event in 2006, associated with windfall from storms during the wet season. Because these fallen trees can take multiple decades to decompose (Hérault et al., 2010), a lag in their contribution to NEE would only be apparent over longer integration times. An additional set of surveys at the Paracou site surrounding Guyaflux, spanning 16 years (1991–2007) in adjacent intact forest plots, found net AGWI accrual of  $0.45 \text{ MgC ha}^{-1} \text{yr}^{-1}$ , primarily in the largest trees (Rutishauser et al., 2010).

Our comparison between MS-PEARL corrected NEE and AGWI is limited because AGWI only quantifies net carbon accumulation or loss in live aboveground woody biomass (including only trees greater than 10 cm diameter), whereas NEE quantifies net carbon accumulation or loss in all ecosystem pools ( $\text{NEE} = -\text{NEP} = -\text{NPP} + \text{heterotrophic } R = -\text{GPP} + \text{autotrophic } R + \text{heterotrophic } R$ ), including other live aboveground biomass (e.g. small trees), live belowground biomass (e.g. roots), and dead biomass (e.g. decaying wood, plant matter and soil).

Complete surveys of fluxes from all carbon pools have accounted comprehensively for NPP, heterotrophic  $R$ , and their difference, NEE, at both tropical sites (Malhi et al., 2009; Rowland et al., 2014). NEE totaled 0.5 and  $-0.3 \text{ MgC ha}^{-1} \text{yr}^{-1}$  for TNF km67 and Guyaflux respectively. Fluxes from individual carbon pools were measured at year-

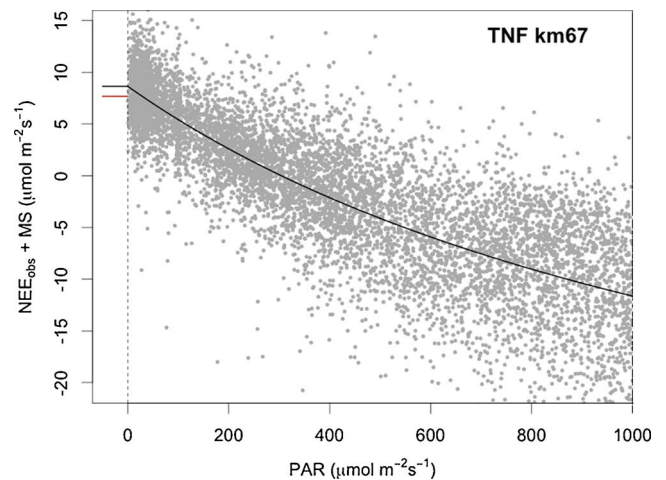


Fig. 7. Evening MS-corrected hourly NEE vs. PAR for PAR > 0 (grey points) at TNF km67. Black line is the best fit nonlinear regression (Eq. (6);  $a_2 = 0$ ). Black line segment to the left of the y-intercept is the respiration parameter  $a_1$ , the limit of evening  $\text{NEE}_{\text{obs}} + \text{MS}$  as PAR approaches zero. Red line segment is mean  $\text{NCE}_{\text{obs}} + \text{MS}$ . The difference between the two line segments is the PEARL estimate for  $A_{\text{night}} = 1.05 \text{ μmol m}^{-2} \text{s}^{-1}$  for TNF km67. (For interpretation of the references to colour in this figure legend, the reader is referred to the web version of this article.)

long or longer intervals, but were non-simultaneous, spanned less than a decade, and had large errors from limited sampling of pools, which compounded to more than  $3 \text{ MgC ha}^{-1} \text{yr}^{-1}$  in aggregate. However, of the individual live and dead carbon pools, these pools only lost or accrued biomass at a rate of less than 15% of AGWI on an annual basis,

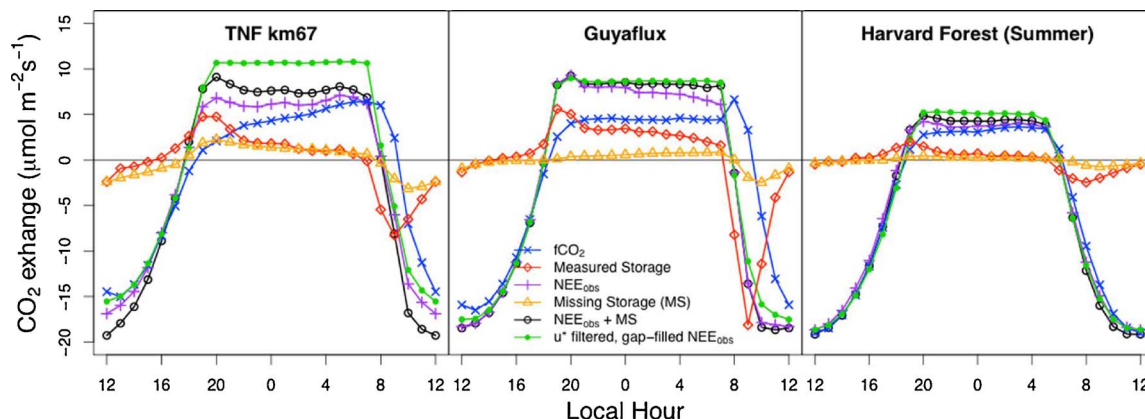


Fig. 6. Mean diurnal cycle of measured fluxes and MS correction.



**Table 3**

Mean advective loss and annual NEE before and after DRAINO and PEARL corrections for each site. 95% confidence intervals in parentheses. For Harvard Forest, the mean annual NEE was only corrected for the summer season MS-PEARL, making this an incomplete correction.

Site	Advective Loss ( $\mu\text{mol m}^{-2} \text{s}^{-1}$ )			Mean Annual NEE ( $\text{MgC ha}^{-1} \text{y}^{-1}$ )			
	CPD $u_*$ filter	DRAINO	PEARL	NEE <sub>obs</sub> no $u_*$ filter	CPD $u_*$ filter	MS-DRAINO	MS-PEARL
TNF km67	3.95 (3.63, 4.01)	0.99	1.05 (0.83, 1.27)	−3.10 (−3.24, −2.94)	4.42 (3.88, 5.08)	−0.94 (−1.10, −0.78)	−0.92 (−1.50, −0.32)
Guyaflux	0.42 (0.40, 0.45)	–	1.91 (1.66, 2.18)	−4.34 (−4.51, −4.15)	−3.49 (−3.70, −3.29)	–	−0.84 (−1.39, −0.30)
Harvard Forest (summer only)	0.73 (0.69, 0.75)	1.36 (1.16, 1.56)	1.69 (1.36, 2.05)	−3.57 (−3.65, −3.50)	−2.96 (−3.04, −2.89)	−2.88 (−3.07, −2.71)	−2.72 (−2.91, −2.51)

with exception to CWD at km67 ( $0.8 \pm 0.9 \text{ MgC ha}^{-1} \text{yr}^{-1}$  annual net loss in 2001–2005) (Rice et al., 2004; Hutyra et al., 2008; Malhi et al., 2009). More recent surveys of the TNF km67 CWD pool, however, indicate that this pool too has equilibrated (Hayek, 2017), with inputs to and losses from this pool being approximately equivalent after 2005 ( $0.02 \pm 0.6 \text{ MgC ha}^{-1} \text{yr}^{-1}$  annual net accrual). An updated whole-forest NEE result for TNF km67 using the equilibrated CWD flux and Malhi et al. (2009) net fluxes for other carbon stocks would therefore be  $-0.3 \text{ MgC ha}^{-1} \text{yr}^{-1}$  (net accrual). Although extensive, simultaneous, and frequent bottom-up inventories of NEE, including all relevant autotrophic and heterotrophic  $R$  fluxes, are challenging, they are a necessary future step to reduce errors and definitively validate the MS-PEARL correction. Nonetheless, the accrual or losses in pools other than AGWB were in aggregate less than the 95% confidence intervals for random measurement errors in our estimates of AGWI. AGWI therefore provides a reasonable means for approximating whole-forest NEE in the case of these two forests. Forest inventories, whether examining the long-term AGWI or shorter-term annual whole-forest NEE, agree with MS-PEARL results that the two tropical forests are in fact slight sinks, closer to carbon-neutral than the CPD  $u_*$ -filter results (Table 3) suggest.

Results for MS-PEARL-corrected mean nighttime  $R$  at the TNF km67 site were consistent with previous literature estimates that applied  $u_*^{Th} = 0.22$  to the first four years of eddy flux data (Hutyra et al., 2007). An independent flux estimate using continuous measurements of Radon-222 ( $^{222}\text{Rn}$ ) as a tracer of  $\text{CO}_2$  exchange (Martens et al., 2004) quantified one full year of  $R$  as  $7.9 \pm 0.8 \mu\text{mol m}^{-2} \text{s}^{-1}$ , which agreed with literature  $R$  ( $u_*^{Th} = 0.22$ ) =  $8.6 \pm 0.1 \mu\text{mol m}^{-2} \text{s}^{-1}$  (Hutyra et al., 2008) and with our MS-PEARL correction  $R = 8.79 \pm 0.26 \mu\text{mol m}^{-2} \text{s}^{-1}$ . An additional three years of eddy flux data, however, resulted in a divergence between NEE<sub>obs</sub> ( $u_*^{Th} = 0.22$ ) and NEE<sub>obs</sub> + MS-PEARL that differs in sign and magnitude (Fig. 8). Our findings therefore do not contradict previous independently verified estimates of the nighttime carbon budget. Rather, as additional eddy covariance data have become available, our results suggest that the  $u_*$  filter paradigm for correction of flux biases has become increasingly in need of replacement.

Provided that our underlying assumptions are correct, the MS-PEARL framework presents a reliable means of correcting selective systematic biases in multi-year NEE records, but it should be used cautiously in analyses (e.g. model-data fusion approaches) at the native hourly resolution of eddy flux measurements. One reason is that empirical parameter fitting in our approach (e.g. Eqs. (3)–(4)) makes MS-corrected measurements more contaminated by empirically modeled output, even more so when combined with typical gap-filling approaches using PAR and temperature regression model outputs (Falge et al., 2001; Dunn et al., 2007; Urbanski et al., 2007). Additionally, estimating advective loss relies on multi-year sets of hourly data used in model fitting (Eq. (6)). The resulting  $A_{\text{night}}$  is a constant offset, providing no information about the inter-hour variability of the advective divergence loss process relative to NEE<sub>obs</sub>.

Small error bounds for the PEARL  $A_{\text{night}}$  estimate depend on very long time series of eddy flux data. For the 10-year record at Paracou,

95% confidence intervals were  $\pm 0.4 \text{ MgC ha}^{-1} \text{y}^{-1}$ . Evaluating this quantity for only the year 2013 increased the error to  $\pm 1.3 \text{ MgC ha}^{-1} \text{y}^{-1}$  due to the smaller sample size. The findings of this study therefore highlight the need for long-term decadal eddy covariance measurement campaigns reduce uncertainties in the net terrestrial carbon balance.

#### 4. Conclusions

Although the  $u_*$  filter has remained the preferred approach to addressing biases in eddy covariance measurements for more than twenty years, results from two tropical forest sites demonstrate that this correction can result in biased hourly nighttime respiration rates and large uncertainty in the long-term ecosystem carbon balance, including sums that are physically unrealistic. The data retention rate can also be very low—as little as 7% at one tropical site. We considered MS as an alternative simple model to the  $u_*$  filter to explain turbulence biases in NCE<sub>obs</sub>. The MS model accounted for slope-plateau behavior of the NCE<sub>obs</sub> vs.  $u_*$  relationship and provided a sensible explanation for the variation in curve shape between sites, without discarding any data.

After correcting NEE<sub>obs</sub> by MS, we have demonstrated that PEARL nocturnal advective divergence loss estimates show good agreement with DRAINO measurements and produce reasonable estimates of long-term carbon balance. PEARL may therefore be an especially effective method for estimating advective divergence loss at sites where direct measurements are not available.

Future investigations are needed into the speculative hypotheses underlying the MS-PEARL and  $u_*$  filter approaches, in order to determine which method has more physically sound hypotheses. Additional work is needed to account for the effects of leaf shedding and snowfall upon MS in the temperate forest dormant season, when both the  $u_*$  filter and MS-PEARL approaches fail. Contingent upon the results of such investigations, the MS-PEARL correction has potential for widespread application to eddy covariance estimates of the long-term carbon balance in global forests.

#### Acknowledgements

This work was supported by funding from a National Science Foundation PIRE fellowship (OISE 0730305) and a U.S. Department of Energy grant (DE-SC0008311). The km67 eddy flux data used in this study are available online via the Oak Ridge National Laboratory (ORNL) Ameriflux network database at [ftp://cdiac.ornl.gov/pub/ameriflux/data/Level2/Sites\\_ByID/BR-Sa1](ftp://cdiac.ornl.gov/pub/ameriflux/data/Level2/Sites_ByID/BR-Sa1). Further site description and data links are available online at ORNL Fluxnet <http://fluxnet.ornl.gov/site/83>.

We thank Benoit Burban who technically manages the Guyaflux site. The Guyaflux program belongs to the SOERE F-ORE-T which is supported annually by Ecofor, Allenvi and the French national research infrastructure ANAEE-F. The Guyaflux program also received support from the “Observatoire du Carbone en Guyane” and an “investissement d’avenir” grant from the Agence Nationale de la Recherche (CEBA, ref

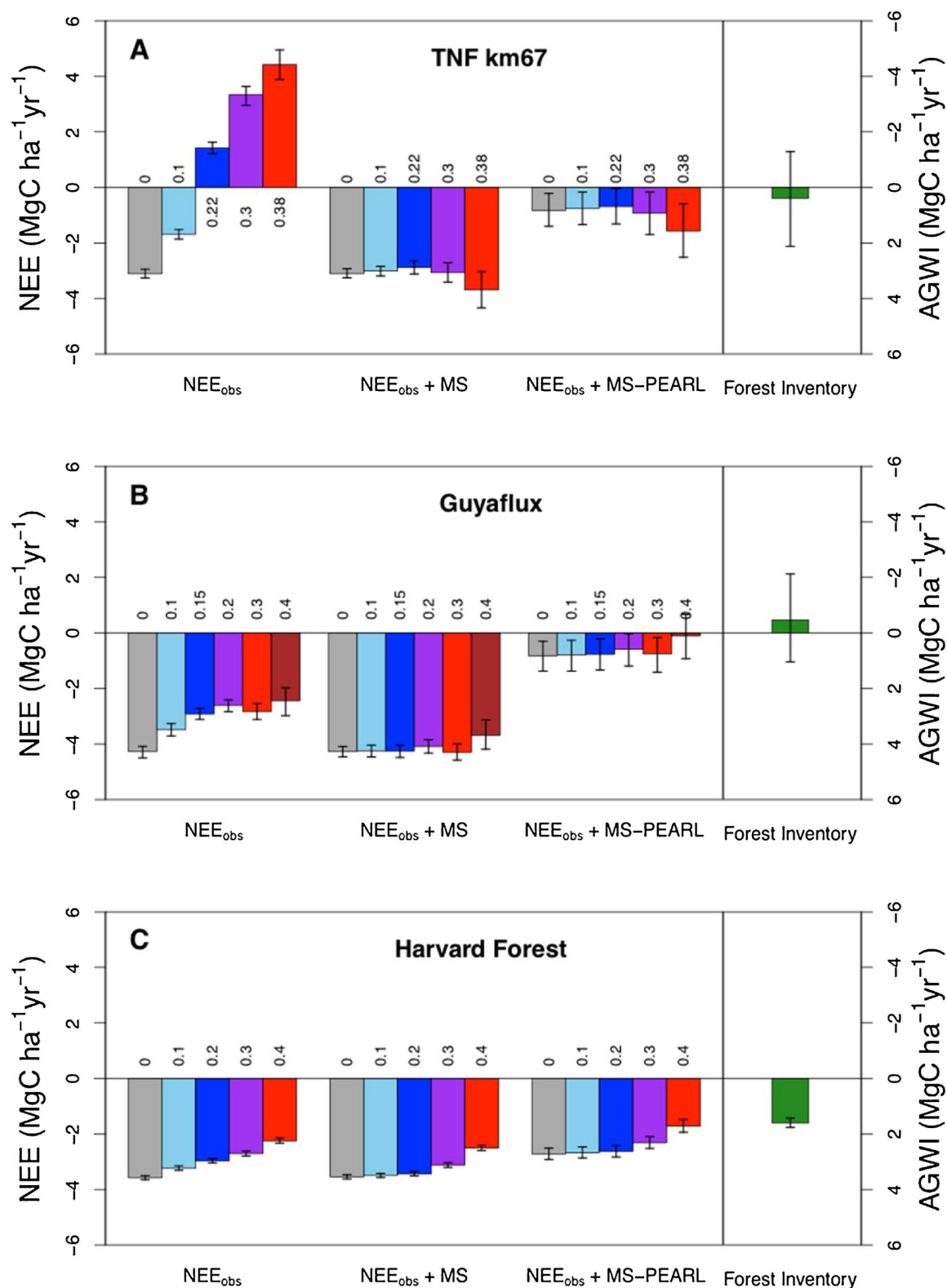


**Fig. 8.** Mean annually integrated NEE with respect to various  $u_*$  filters ( $u_*^{\text{Th}}$  above or below bars) for each stage of the MS-PEARL correction, compared with AGWI derived from forest inventories for (A) TNF km67 (B) Guyaflux (C) Harvard Forest. For Harvard Forest, the MS and PEARL corrections were not applied for the full year, only the growing season, because no  $u_*^{\text{Th}}$  could be found during the dormant season and so the MS correction could not be reliably implemented. Error bars represent 95% bootstrap confidence intervals, representing hourly random measurement errors on mean annual estimates.

ANR-10-LABX-25-01).

## Appendix A. Supplementary data

Supplementary data associated with this article can be found, in the online version, at <https://doi.org/10.1016/j.agrformet.2017.12.186>.

## References

- Acevedo, O., Moraes, O., Degrazia, G., Fitzjarrald, D., Manzi, A., Campos, J., 2009. Is friction velocity the most appropriate scale for correcting nocturnal carbon dioxide fluxes? *Agric. For. Meteorol.* 149, 1–10. <http://dx.doi.org/10.1016/j.agrformet.2008.06.014>.
- Aubinet, M., Heinesch, B., Yernaux, M., 2003. Horizontal and vertical CO<sub>2</sub> advection in a sloping forest. *Bound. Layer Meteorol.* 108, 397–417. <http://dx.doi.org/10.1023/A:1024168428135>.
- Aubinet, M., Feigenwinter, C., Heinesch, B., Bernhofer, C., Canepa, E., Lindroth, A., Montagnani, L., Rebmann, C., Sedlak, P., Van Gorsel, E., 2010. Direct advection measurements do not help to solve the night-time CO<sub>2</sub> closure problem: evidence from three different forests. *Agric. For. Meteorol.* 150, 655–664. <http://dx.doi.org/10.1016/j.agrformet.2010.01.016>.
- Bain, W.G., Hutrya, L., Patterson, D.C., Bright, A.V., Daube, B.C., Munger, J.W., Wofsy, S.C., 2005. Wind-induced error in the measurement of soil respiration using closed dynamic chambers. *Agric. For. Meteorol.* 131, 225–232. <http://dx.doi.org/10.1016/j.agrformet.2005.06.004>.
- Barr, A.G., Richardson, A.D., Hollinger, D.Y., Papale, D., Arain, A., Black, T.A., Bohrer, G., Dragoni, D., Fischer, M.L., Gu, L., Law, B.E., Margolis, H.A., McCaughy, J.H., Munger, J.W., Oechel, W., Schaeffer, K., 2013. Use of change-point detection for friction-velocity threshold evaluation in eddy-covariance studies. *Agric. For. Meteorol.* 171–172, 31–45. <http://dx.doi.org/10.1016/j.agrformet.2012.11.023>.
- Bonal, D., Bosc, A., Ponton, S., Goret, J.-Y., Burban, B., Gross, P., Bonnefond, J.-M., Elbers, J., Longdoz, B., Epron, D., Guehl, J.-M., Granier, A., 2008. Impact of severe dry season on net ecosystem exchange in the Neotropical rainforest of French Guiana. *Glob. Change Biol.* 14, 1917–1933. <http://dx.doi.org/10.1111/j.1365-2486.2008.01610.x>.
- Bruhn, D., Mikkelsen, T.N., Herbst, M., Kutsch, W.L., Ball, M.C., Pilegaard, K., 2011. Estimating daytime ecosystem respiration from eddy-flux data. *Biosystems* 103, 309–313. <http://dx.doi.org/10.1016/j.biosystems.2010.10.007>.
- Dunn, A.L., Barford, C.C., Wofsy, S.C., Goulden, M.L., Daube, B.C., 2007. A long-term record of carbon exchange in a boreal black spruce forest: means, responses to interannual variability, and decadal trends. *Glob. Change Biol.* 13, 577–590. <http://dx.doi.org/10.1111/j.1365-2486.2006.01221.x>.
- Falge, E., Baldocchi, D., Olson, R., Anthoni, P., Aubinet, M., Bernhofer, C., Burba, G., Ceulemans, R., Clement, R., Dolman, H., Granier, A., Gross, P., Grünwald, T., Hollinger, D., Jensen, N.-O., Katul, G., Keronen, P., Kowalski, A., Lai, C.T., Law, B.E., Meyers, T., Moncrieff, J., Moors, E., Munger, J.W., Pilegaard, K., Rannik, Ü., Rebmann, C., Suyker, A., Tenhunen, J., Tu, K., Verma, S., Vesala, T., Wilson, K., Wofsy, S., 2001. Gap filling strategies for defensible annual sums of net ecosystem exchange. *Agric. For. Meteorol.* 107, 43–69. [http://dx.doi.org/10.1016/S0168-1923\(00\)00225-2](http://dx.doi.org/10.1016/S0168-1923(00)00225-2).
- Galvagno, M., Wohlfahrt, G., Cremonese, E., Filippa, G., Migliavacca, M., Mora, U., Cella, D., Van Gorsel, E., 2017. Contribution of advection to nighttime ecosystem respiration at a mountain grassland in complex terrain. *Agric. For. Meteorol.* 270–281, 270–281. <http://dx.doi.org/10.1016/j.agrformet.2017.02.018>.
- Giasson, M.-A., Ellison, A.M., Bowden, R.D., Crill, P.M., Davidson, E.A., Drake, J.E., Frey, S.D., Hadley, J.L., Lavine, M., Melillo, J.M., Munger, J.W., Nadelhoffer, K.J., Nicoll, L., Ollinger, S.V., Savage, K.E., Steudler, P.A., Tang, J., Varner, R.K., Wofsy, S.C., Foster, D.R., Finzi, A.C., 2013. Soil respiration in a northeastern US temperate forest: a 22-year synthesis. *Ecosphere* 4, 1–28. <http://dx.doi.org/10.1890/ES13.00183.1>.
- Goulden, M.L., Munger, J.W., Fan, S.-M., Daube, B.C., Wofsy, S.C., 1996. Measurements of carbon sequestration by long-term eddy covariance: methods and a critical evaluation of accuracy. *Glob. Change Biol. [Global Change Biol.]* 2, 169–182. <http://dx.doi.org/10.1111/j.1365-2486.1996.tb00070.x>.
- Grace, J., Malhi, Y., Lloyd, J., McIntyre, J., Miranda, A.C., Meir, P., Miranda, H.S., 1996. The use of eddy covariance to infer the net carbon dioxide uptake of Brazilian rain forest. *Glob. Chang Biol.* 2, 209–217. <http://dx.doi.org/10.1111/j.1365-2486.1996.tb00073.x>.
- Gu, L., Baldocchi, D., Verma, S.B., Black, T.A., Vesala, T., Falge, E.M., Dowty, P.R., 2002. Advantages of diffuse radiation for terrestrial ecosystem productivity. *J. Geophys. Res.* Atmos. 107, ACL2-1. <http://dx.doi.org/10.1029/2001JD001242>.
- Gu, L., Falge, E., Boden, T., Baldocchi, D., Black, T., Saleska, S., Suni, T., Verma, S., Vesala, T., Wofsy, S., 2005. Objective threshold determination for nighttime eddy flux filtering. *Agric. For. Meteorol.* 128, 179–197. <http://dx.doi.org/10.1016/j.agrformet.2004.11.006>.
- Héroult, B., Beauchêne, J., Muller, F., Wagner, F., Baraloto, C., Blanc, L., Martin, J.-M., 2010. Modeling decay rates of dead wood in a neotropical forest. *Oecologia* 164, 243–251. <http://dx.doi.org/10.1007/s00442-010-1602-8>.
- Hayek, M., 2017. Drivers of Long-Term Variability in Amazon Forest Carbon Fluxes. Doctoral Dissertation. Harvard University.
- Heskel, M.A., Atkin, O.K., Turnbull, M.H., Griffin, K.L., 2013. Bringing the Kok effect to light: a review on the integration of daytime respiration and net ecosystem exchange. *Ecosphere* 4, 1–14. <http://dx.doi.org/10.1890/ES13-00120.1>.
- Hutrya, L.R., Munger, J.W., Saleska, S.R., Gottlieb, E., Daube, B.C., Dunn, A.L., Amaral, D.F., de Camargo, P.B., Wofsy, S.C., 2007. Seasonal controls on the exchange of carbon and water in an Amazonian rain forest. *J. Geophys. Res. Biogeosci.* 112, G03008. <http://dx.doi.org/10.1029/2006JG000365>.
- Hutrya, L.R., Munger, J.W., Hammond-Pyle, E., Saleska, S.R., Restrepo-Coupe, N., Daube, B.C., de Camargo, P.B., Wofsy, S.C., 2008. Resolving systematic errors in estimates of net ecosystem exchange of CO<sub>2</sub> and ecosystem respiration in a tropical forest biome. *Agric. For. Meteorol.* 148, 1266–1279. <http://dx.doi.org/10.1016/j.agrformet.2008.03.007>.
- IPCC, 2013. Summary for policymakers. In: Stocker, T.F., Qin, D., Plattner, G.-K., Tignor, M., Allen, S.K., Boschung, J., Nauels, A., Xia, Y., Bex, V., Midgley, P.M. (Eds.), *Climate Change 2013: the Physical Science Basis. Contribution of Working Group I to the Fifth Assessment Report of the Intergovernmental Panel on Climate Change*. Cambridge Univ. Press Cambridge, UK and New York, NY, USA, pp. 1–33.
- Lee, X., 1998. On micrometeorological observations of surface-air exchange over tall vegetation. *Agric. For. Meteorol.* 91, 39–49. [http://dx.doi.org/10.1016/S0168-1923\(98\)00071-9](http://dx.doi.org/10.1016/S0168-1923(98)00071-9).
- Malhi, Y., Saatchi, S., Girardin, C., Aragão, L.E.O.C., 2009. The production, storage, and flow of carbon in Amazonian forests. *Amazonia and Global Change*. pp. 355–372. <http://dx.doi.org/10.1029/2008GM000779>.
- Martens, C., Shay, T., Mendlovitz, H., Matross, D., Saleska, S., Wofsy, S., Woodward, S., Mentons, M., Moura, J., Crill, P., De Moraes, O., Lima, R., 2004. Radon fluxes in tropical forest ecosystems of Brazilian Amazonia: night-time CO<sub>2</sub> net ecosystem exchange derived from radon and eddy covariance methods. *Glob. Change Biol.* 618–629. <http://dx.doi.org/10.1111/j.1529-8817.2003.00764.x>.
- Miller, S.D., Goulden, M.L., Menton, M.C., Da Rocha, H.R., De Freitas, H.C.E., Silva Figueira, A.M., De Sousa, C.A.D., 2004. Biometric and micrometeorological measurements of tropical forest carbon balance. *Ecol. Appl.* 14, 114–126. <http://dx.doi.org/10.1890/02-6005>.
- Moncrieff, J.B., Malhi, Y., Leuning, R., Mahli, Y., Leuning, R., 1996. The propagation of errors in long-term measurements of land-atmosphere fluxes of carbon and water. *Glob. Change Biol.* 2, 231–240. <http://dx.doi.org/10.1111/j.1365-2486.1996.tb00075.x>.
- Papale, D., Reichstein, M., Aubinet, M., Canfora, E., Bernhofer, C., Kutsch, W., Longdoz, B., Rambal, S., Valentini, R., Vesala, T., Yakir, D., 2006. Towards a standardized processing of net ecosystem exchange measured with eddy covariance technique: algorithms and uncertainty estimation. *Biogeosciences* 3, 571–583. <http://dx.doi.org/10.5194/bg-3-571-2006>.
- Phillips, S.C., Varner, R.K., Frolking, S., Munger, J.W., Bubier, J.L., Wofsy, S.C., Crill, P.M., 2010. Interannual, seasonal, and diel variation in soil respiration relative to ecosystem respiration at a wetland to upland slope at Harvard Forest. *J. Geophys. Res.* 115, 1–18. <http://dx.doi.org/10.1029/2008JG000858>.
- Phillips, C.L., Nickerson, N., Risk, D., Bond, B.J., 2011. Interpreting diel hysteresis between soil respiration and temperature. *Glob. Change Biol.* 17, 515–527. <http://dx.doi.org/10.1111/j.1365-2486.2010.02250.x>.
- Pyle, E.H., Santoni, G.W., Nascimento, H.E.M., Hutrya, L.R., Vieira, S., Curran, D.J., Van Haren, J., Saleska, S.R., Chow, V.Y., Camargo, P.B., Laurance, W.F., Wofsy, S.C., 2009. Dynamics of carbon, biomass, and structure in two Amazonian forests. *J. Geophys. Res.* 114. <http://dx.doi.org/10.1029/2007JG000592>.
- Reichstein, M., Falge, E., Baldocchi, D., Papale, D., Aubinet, M., Berbigier, P., Bernhofer, C., Buchmann, N., Gilmanov, T., Granier, A., Gr??nwald, T., Havr??nkov??, K., Ilvesniemi, H., Janous, D., Knohl, A., Laurila, T., Lohila, A., Loustau, D., Matteucci, G., Meyers, T., Miglietta, F., Ourcival, J.M., Pumpanen, J., Rambal, S., Rotenberg, E., Sanz, M., Tenhunen, J., Seufert, G., Vaccari, F., Vesala, T., Yakir, D., Valentini, R., 2005. On the separation of net ecosystem exchange into assimilation and ecosystem respiration: review and improved algorithm. *Glob. Change Biol.* 11, 1424–1439. <http://dx.doi.org/10.1111/j.1365-2486.2005.001002.x>.
- Rice, A.H., Pyle, E.H., Saleska, S.R., Hutrya, L., Palace, M., Keller, M., de Camargo, P.B., Portillo, K., Marques, D.F., Wofsy, S.C., 2004. Carbon balance and vegetation dynamics in an old-growth Amazonian forest. *Ecol. Appl.* 14, 55–71. <http://dx.doi.org/10.1890/02-6006>.
- Rowland, L., Hill, T.C., Stahl, C., Siebicke, L., Burban, B., Zaragoza-Castells, J., Ponton, S., Bonal, D., Meir, P., Williams, M., 2014. Evidence for strong seasonality in the carbon storage and carbon use efficiency of an Amazonian forest. *Glob. Change Biol.* 20, 979–991. <http://dx.doi.org/10.1111/gcb.12375>.
- Rutishauser, E., Wagner, F., Herault, B., Nicolini, E.A., Blanc, L., 2010. Contrasting above-ground biomass balance in a Neotropical rain forest. *J. Veg. Sci.* 21, 672–682. <http://dx.doi.org/10.1111/j.1654-1103.2010.01175.x>.
- Saleska, S.R., Miller, S.D., Matross, D.M., Goulden, M.L., Wofsy, S.C., da Rocha, H.R., de Camargo, P.B., Crill, P., Daube, B.C., de Freitas, H.C., Hutrya, L., Keller, M., Kirchhoff, V., Menton, M., Munger, J.W., Pyle, E.H., Rice, A.H., Silva, H., 2003. Carbon in Amazon forests: unexpected seasonal fluxes and disturbance-induced losses. *Science* 302, 1554–1557. <http://dx.doi.org/10.1126/science.1091165>.
- Staeble, R.M., Fitzjarrald, D.R., 2004. Observing subcanopy CO<sub>2</sub> advection. *Agric. For. Meteorol.* 122, 139–156. <http://dx.doi.org/10.1016/j.agrformet.2003.09.011>.
- Staeble, R.M., Fitzjarrald, D.R., 2005. Measuring canopy structure and the kinematics of subcanopy flows in two forests. *J. Appl. Meteorol.* 44, 1161–1179. <http://dx.doi.org/10.1175/JAM2265.1>.
- Sun, J., Desjardins, R.L., Mahrt, L., MacPherson, J.L., 1998. Transport of carbon dioxide, water vapor, and ozone by turbulence and local circulations. *J. Geophys. Res.* 103, 25873–25885. <http://dx.doi.org/10.1029/98JD02439>.
- Tóta, J., Fitzjarrald, D.R., Staeble, R.M., Sakai, R.K., Moraes, O.M.M., Acevedo, O.C., Wofsy, S.C., Manzi, A.O., 2008. Amazon rain forest subcanopy flow and the carbon budget: santarém LBA-ECO site. *J. Geophys. Res. Biogeosci.* 113. <http://dx.doi.org/10.1029/2007JG000597>. n/a-n/a.
- Tóta, J., Roy Fitzjarrald, D., da Silva Dias, M.A.F., 2012. Amazon rainforest exchange of carbon and subcanopy air flow: manaus LBA site—A complex terrain condition. *Sci.*

- World J. 2012, 1–19. <http://dx.doi.org/10.1100/2012/165067>.
- Urbanski, S., Barford, C., Wofsy, S., Kucharik, C., Pyle, E., Budney, J., McKain, K., Fitzjarrald, D., Czikowsky, M., Munger, J.W., 2007. Factors controlling CO<sub>2</sub> exchange on timescales from hourly to decadal at Harvard Forest. *J. Geophys. Res. Biogeosci.* 112, G02020. <http://dx.doi.org/10.1029/2006JG000293>.
- Wofsy, S.C., Goulden, M.L., Munger, J.W., Fan, S.M., Bakwin, P.S., Daube, B.C., Bassow, S.L., Bazzaz, F.a., 1993. Net exchange of C in a mid-latitude forest. *Science* 80, O2. <http://dx.doi.org/10.1126/science.260.5112.1314>.
- van Gorsel, E., Leuning, R., Cleugh, H.A., Keith, H., Suni, T., 2007. Nocturnal carbon efflux: reconciliation of eddy covariance and chamber measurements using an alternative to the  $u^*$  – threshold filtering technique. *Tellus Ser. B Chem. Phys. Meteorol.* 59, 397–403. <http://dx.doi.org/10.1111/j.1600-0889.2007.00252.x>.
- van Gorsel, E., Leuning, R., Cleugh, H.A., Keith, H., Kirschbaum, M.U.F., Suni, T., 2008. Application of an alternative method to derive reliable estimates of nighttime respiration from eddy covariance measurements in moderately complex topography. *Agric. For. Meteorol.* 148, 1174–1180. <http://dx.doi.org/10.1016/j.agrformet.2008.01.015>.